Ecological Indicators 111 (2020) 106042

Contents lists available at ScienceDirect

Ecological Indicators

journal homepage: www.elsevier.com/locate/ecolind

# Spectral responses to labile organic carbon fractions as useful soil quality indicators across a climatic gradient

Paulina B. Ramírez[a], Francisco J. Calderón[b], Steven J. Fonte[c], Fernando Santibáñez[d], Carlos A. Bonilla[a,e,*]

[a] Departamento de Ingeniería Hidráulica y Ambiental, Pontificia Universidad Católica de Chile, Av. Vicuña Mackenna 4860, Macul, Santiago 7820436, Chile
[b] Central Great Plains Research Station USDA–ARS, Akron, CO 80720, USA
[c] Department of Soil and Crop Sciences, Colorado State University, Fort Collins, CO 80523, USA
[d] Departamento de Ingeniería y Suelos, Universidad de Chile, Casilla 1004, Santiago, Chile
[e] Centro de Desarrollo Urbano Sustentable CONICYT/FONDAP/15110020, El Comendador 1916, Providencia, Santiago 7520245, Chile

ARTICLE INFO

*Keywords:*
Alkyl C
Chile
Infrared spectroscopy
light fraction (LF)
permanganate oxidizable carbon (POXC)
Soil carbon

ABSTRACT

Light fraction (LF) and permanganate-oxidizable C (POXC) demonstrate high reliability as indicators for monitoring soil functioning in response to changes in soil organic carbon (SOC). However, mechanisms affecting the amount and composition of labile fractions and their relationship with SOC content at regional scales have not been thoroughly studied. The aim of this study was to examine the spectral features associated with these labile organic matter fractions in samples collected from 75 sites under different soil types, land use and climatic conditions in Chile. Topsoil was analyzed for total C and N content, aggregate stability, and texture. Additionally, the spectral properties of LF material and whole soils were analyzed using diffuse reflectance mid-infrared spectroscopy (MidIR). Our results show that LF shared a similar spectral composition but with different band intensities across climatic regimes. LF spectra were associated with O-alkyl C in cool and rainy areas, whereas a relative accumulation of aromatic structures was found in warmer areas. Whole soils spectra showed that SOC, POXC and aggregability were related to the prevalence of aliphatic and polysaccharides compounds in colder areas. While in warm arid areas, the stabilization of aliphatic compounds was found to be related to clay minerals. Furthermore, we found that POXC and SOC content were closely related and changes in POXC were affected by variations in climate conditions. The understanding of spectral features linked to labile SOC fractions on at larger geographical scale will contribute to the development of sustainable land management options for the prevention of land degradation in the context of adaptation to climate change.

## 1. Introduction

The dynamics and quality of soil organic carbon (SOC) are essential to a variety of important soil functions and ecosystem services (Lal, 2016; Lefèvre et al., 2017). Adopting soil conservation practices such as to minimize soil disturbance, use of crop residues, and cropping systems diversification leads to increasing SOC contents and a long-term agroecosystem sustainability (Lal, 2004). However, this is not straightforward as climate condition may alter SOC responses to agricultural practices and land use (Dimassi et al., 2014; Hermle et al., 2008). Thus, it is necessary to explore indicators sensitive to alterations in soil quality to determine whether a changing climate could impact SOC.

Labile SOC fractions that account for a small, but reactive proportion of SOM (Haynes, 2005; Poirier et al., 2005; Verma et al., 2013; Yan et al., 2007). Labile SOC fractions have been suggested as early indicators of the effects of soil management and cropping systems on SOM quality (Denef et al., 2007; Gregorich and Ellert, 1993; Haynes, 2005). For example, light fraction (LF) and permanganate oxidizable C (POXC) have been suggested to respond to land use change in the short-term and have been used to detect the effects of different land management practices. (Culman et al., 2012; Duval et al., 2018; Gregorich et al., 1994; Hurisso et al., 2016). The occurrence of permanganate oxidizable carbon (POXC) by a mild oxidizing agent $KMnO_4$ represent a promising, and inexpensive indicator for soil health assessment, which is associated with the loss of organic matter as an oxidative process

* Corresponding author at: Departamento de Ingeniería Hidráulica y Ambiental, Pontificia Universidad Católica de Chile, Av. Vicuña Mackenna 4860, Macul, Santiago 7820436, Chile.
*E-mail address:* cbonilla@ing.puc.cl (C.A. Bonilla).

https://doi.org/10.1016/j.ecolind.2019.106042
Received 3 July 2019; Received in revised form 17 December 2019; Accepted 23 December 2019
Available online 03 January 2020
1470-160X/ © 2020 Elsevier Ltd. All rights reserved.

comparable to those in microbial oxidation (Blair et al., 1995; Conteh et al., 1999). In addition, LF material consists largely of undecomposed or partly decomposed root and plant fragments that responds more rapidly to the effects of management practices (Biederbeck et al., 1994; Cambardella and Elliott, 1992; Golchin et al., 1994; Gregorich and Janzen, 1996), and primarily associated with readily decomposable substrate for soil microorganisms as well as soil carbon formation(Song et al., 2012).

A wide variety of analytical methods have been used to measure labile fractions, most of which are based on its physical, chemical, and biochemical principles (Strosser, 2010). However, these procedures are usually more time consuming, and thus infrared spectroscopy has been proposed as an alternative method for a rapid determination of soil quality (Comino et al., 2018; Summers et al., 2011). Fourier-transformed mid-infrared (MidIR) spectroscopy has been widely applied to characterize organic matter in soils and predict the distribution of SOC fractions (Leifeld, 2006; Madhavan et al., 2017; Viscarra Rossel et al., 2006). Specific MidIR absorbance bands typically associated with aliphatics, methyls, amides III, and polysaccharides in specific soils can be ascribed to labile SOC (Calderón et al., 2017; Peltre et al., 2014). Thus, MidIR could be used to predict SOC fraction distribution and composition as well as an evaluation tools complementing traditional quality indicators.

According to the chemical convergence hypothesis, all changes in chemistry during litter decomposition result from the preferential loss of easily degradable compounds (e.g. starch and proteins) and the relative accumulation of compounds that are more resistant to decay (Wickings et al., 2012). Thus, chemically distinct litter types pass through the decomposer 'funnel' and may converge towards similar chemistries (Bradford et al., 2016; Moore et al., 2011; Wickings et al., 2012). For example, O-alkyl loss is followed by aromatic breakdown and stabilization of alkyl-C (Wickings et al., 2012). Although it is well understood that variations in ecosystem properties are related to differences in the chemical complexity of SOM, which enables changes in functional group chemistry (Hsu and Lo, 1999; Lützow et al., 2006; Roth et al., 2019), little is known about how variations in LF composition and its sequence of chemical changes are linked to different geographic, climatic, land use and edaphic factors. Therefore, understanding the environmental persistence of the chemically distinct compounds in LF material might be a valuable indicator to elucidate soil C turnover mechanisms and trace the effects ecosystem disturbances on soil quality.

Although labile SOC fractions have emerged as standardized indicators of SOC changes, their chemical composition and regional scale variation has not been extensively studied. The impact of environmental conditions on labile SOM pools and soil properties has largely been determined by separate studies only at a local scale. It is possible that SOC prevalence is largely controlled by the inherent chemical composition of labile fractions or that it follows a common sequence of chemical changes mainly controlled by environmental factors. Thus, the objectives of this study were to: i) to analyze the spectral characteristics of LF material across a range of climates, ii) to determine patterns of chemical functional groups in LF and whole soils under different land use and climate variability, and iii) to evaluate the use of LF and POXC as quality indicators for climate impacts on soil.

## 2. Materials and methods

### 2.1. Study area

Soils were analyzed from 75 different sites with varying soil types and climate conditions along a latitudinal transect in Chile. This study was conducted across a 2000 km transect, from 32°00′ S to 51°00′ S, spanning from the semiarid central region of Chile to the far rainy south (Fig. 1). In the study area, arid, semiarid and subhumid conditions are dominated by Mollisols, Inceptisols followed by Alfisols and Entisols. In humid and hyper humid conditions, Andean foothill are characterized by presence of Andisols with high SOC content (about 110 g C $kg^{-1}$ soil) and Alfisols, Ultisols and Inceptisols between the Andes and the coastal range (Bonilla and Johnson, 2012; Ramírez et al., 2019). Torres del Paine, in the southern Chilean Patagonia, is dominated by Entisols and Inceptisols on younger post-glacial areas, and Histosols in high slope areas (Casanova et al., 2013; Pfeiffer et al., 2010).

### 2.2. Climate data

In general, climates associated with the sites used in this study are characterized by concentrated rainfall during the southern hemisphere's winter season (June to September) and a drier summer season (Bonilla and Vidal, 2011; Lobo et al., 2015). Sites were categorized according to aridity regime (UNESCO, 2010), calculated as the ratio of mean annual precipitation (MAP) to potential evapotranspiration (ET) (UNEP, 1997, 1992), and also by considering the length of the dry season. Climate information was obtained from two different

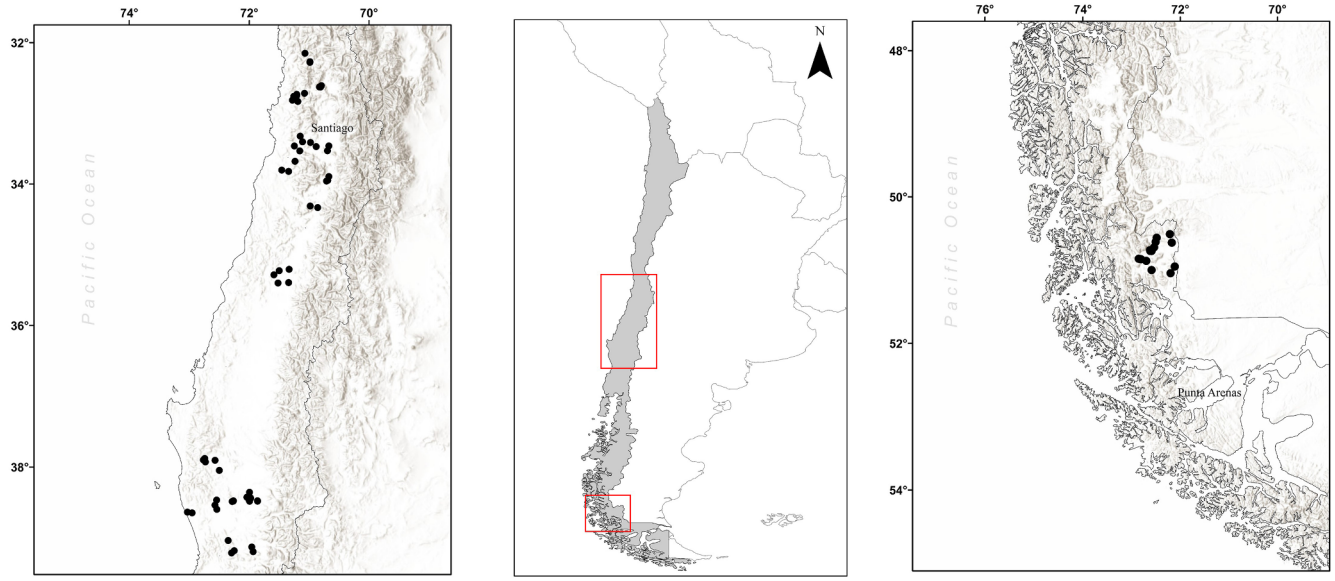


**Fig. 1.** Map of sampling sites in central Chile (left) and southern Chile, Torres de Paine (right). A general view of the study area is shown in the middle.

**Table 1**
Mean values and standard deviations of climate and soil properties of different soils grouped into aridity regimes and land use.

| | | Climate parameters[c] | | | | Soil physico-chemical properties | | | | | |
|---|---|---|---|---|---|---|---|---|---|---|---|
| | n[b] | AI | MAP | MAT | ET | Depth | Sand | Silt | Clay | C:N | pH |
| | | (MAP/ET) | (mm) | (°C) | (mm) | (cm) | (%) | (%) | (%) | | |
| Aridity regime[a] | | | | | | | | | | | |
| Arid | 6 | 0.05–0.20 | 214 ± 125 | 15.0 ± 0.6 | 1201 ± 58 | 18 ± 3 | 42 ± 16 | 34 ± 9 | 24 ± 8 | 18 ± 3 | 7.7 ± 0.2 |
| Semiarid | 22 | 0.20–0.5 | 384 ± 172 | 14.8 ± 0.5 | 1037 ± 37 | 18 ± 4 | 41 ± 19 | 32 ± 10 | 28 ± 10 | 21 ± 7 | 7.3 ± 0.6 |
| Subhumid | 5 | 0.5–1 | 630 ± 208 | 14.4 ± 0.5 | 982 ± 74 | 19 ± 3 | 41 ± 17 | 35 ± 12 | 24 ± 7 | 16 ± 3 | 6.2 ± 0.4 |
| Humid | 9 | 1–1.7 | 1011 ± 192 | 12.3 ± 0.4 | 706 ± 33 | 18 ± 3 | 43 ± 16 | 30 ± 8 | 27 ± 14 | 17 ± 2 | 5.5 ± 0.2 |
| Hyper humid | 17 | > 1.7 | 2094 ± 377 | 12.2 ± 0.4 | 700 ± 39 | 16 ± 3 | 44 ± 11 | 37 ± 10 | 19 ± 9 | 16 ± 4 | 5.7 ± 0.3 |
| Cold semiarid[d] | 16 | 0.20–0.5 | 250 ± 133 | 7.7 ± 0.4 | 875 ± 75 | 20 ± 0 | 45 ± 11 | 40 ± 9 | 16 ± 6 | 11 ± 4 | 6.0 ± 0.6 |
| Land use[d] | | | | | | | | | | | |
| Native forest | 2 | | – | – | | 19 ± 2 | 43 ± 15 | 37 ± 8 | 20 ± 9 | 15 ± 3 | 5.6 ± 0.2 |
| Natural prairie | 14 | | – | – | | 20 ± 0 | 46 ± 9 | 39 ± 9 | 15 ± 4 | 11 ± 5 | 6.1 ± 0.7 |
| Non-cultivated | 15 | | – | – | | 17 ± 4 | 40 ± 15 | 33 ± 8 | 27 ± 9 | 15 ± 4 | 6.6 ± 1.1 |
| Cultivated | 32 | | – | – | | 17 ± 4 | 40 ± 18 | 34 ± 11 | 27 ± 9 | 17 ± 3 | 6.6 ± 0.9 |
| Woody perennial | 4 | | – | – | | 19 ± 1 | 39 ± 22 | 32 ± 11 | 30 ± 17 | 17 ± 4 | 6.4 ± 0.9 |

AI: aridity index; MAT: mean annual temperature; MAP: mean annual precipitation; ET: evapotranspiration; C:N: carbon/nitrogen
[a] aridity regime, defined by the aridity index based on UNEP (1992) and UNESCO (2010).
[b] n, number of sites per group.
[c] Standard deviation in 35 years of data.
[d] Standard deviation in 4 years of data.

meteorological stations, General Directorate of Water (DGA) and National Institute of Agriculture Research (INIA); all the stations were in the vicinity of soil sampling sites. The mean annual temperature (MAT), MAP, and ET of each site are shown in Table 1.

### 2.3. Land use

Sites were located in multiple types of land use areas including a biosphere reserve (Torres del Paine), natural sites, and cultivated sites. Agricultural sites were selected to represent a large range of different C contents based on the official national soil repository data from the Chilean Natural Resources Information Center (CIREN). The CIREN sites were relocated with GPS, and interviews with local farmers and satellite imagery interpretation were applied to collect data on the land use history of each site. The land uses were sorted into five categories: 1) Native forest (NF) classified by the presence of Patagonian oak (*Lophozonia obliqua*) and Lenga (*Nothofagus pumilio*), 2) Natural prairie (NP) comprised of sites in the Patagonian Steppe, inhabited by desert shrubs and tuft grasses, 3) Woody perennial (WP) sites, including forest plantations, orchard or vineyards for at least 7 years, 4) Cultivated (C) sites planted with cereals and/or vegetables for at least 20 years and 5) Non-cultivated (NC) sites were those previously cultivated, but they were under non-agricultural activity or resulted in the development of secondary vegetation succession following cropland abandonment for at least 5 years. Soil physico-chemical properties are listed in Table 1 according to climatic regimes and land use.

### 2.4. Soil sampling and physico-chemical analysis

A total of 75 sites were sampled between January and February over four years (2013, 2014, 2016, and 2017). At each sampling site, two replicate samples were taken randomly at a distance of 100 m from one another. Before soils were collected from the topsoil horizon, plant residue and O horizon were removed. Depending on the site, soils were collected using a soil auger (20 cm diameter) based on the depth of the first horizon ranged from 8 to 29 cm. Genetic horizons were used instead of a fixed soil depth because it offers a better comparison for the processes involved in SOC dynamics (Grüneberg et al., 2010).

For physico-chemical analysis, samples were air-dried and sieved (2 mm). The SOC was determined by potassium dichromate ($K_2Cr_2O_7$) oxidation (Walkley and Black, 1934). The pH was measured in a 1:2.5 soil/water suspension (Sadsawka et al., 2006). Because of the relevance of $CaCO_3$ in calcareous soils, all samples were pre-tested with HCl followed by observation for effervescence to determine if carbonates were present. Subsequently, soil samples were treated with 2 M $H_2SO_4$ containing 2% $FeSO_4.7H_20$ to remove all the carbonate (Nelson and Sommer, 1982). Despite this, non- significant differences in C content were found when using Walkley and Black method between samples with or without $CaCO_3$ removal. Particle size distribution (clay, silt, sand) was measured using the hydrometer method (Gee and Bauder, 1986). Total N was measured using the Kjeldahl digestion method. Finally, water stable aggregates (WSA) were measured using a wet-sieving apparatus (Eijkelkamp, Giesbeek, Netherlands) and were quantified as the proportional mass of stable aggregates in the 1–2 mm range relative to the mass of the whole soil, as presented by Kemper and Rosenau (1986).

### 2.5. Labile SOC fractions

Soil POXC was measured in duplicate using the methodology described by Weil et al. (2003). Briefly, 2.5 g of air-dried and sieved soil were added into propylene tubes with 18 mL of deionized water and 2 mL of 0.2 M $KMnO_4$. The tubes were shaken vigorously for 2 min at 240 oscillations/min. The tubes were allowed to settle for 10 min in dark at room temperature. For stopping the reaction, 0.5 mL of solution was taken from the tube and placed in another tube with 49.5 mL of deionized water, allowing the reaction to end. The absorbance of each sample was measure at 550 nm using a Pocket Colorimeter™ II (HACH Company, USA). The POXC fraction (mg/kg) was calculated as:

$$POXC_{mg/kg} = [0.02\ \text{mol}\ L^{-1} - (a + b \times Abs)] \times (9000\ \text{mg}\ C\ \text{mol}^{-1}) \times (0.02\ L\ \text{solution} \times Wt^{-1})$$

where $0.02 mol L^{-1}$ is the concentration of the $K_2MnO_4$ solution, a is the intercept and b is the slope of the standard calibration curve, 9000mg is the amount of carbon oxidized by 1 mol of MnO4 changing from $Mn^{+7}$ to $Mn^{+4}$, 0.02L is the volume of the $K_2MnO_4$ reacting with the samples, and Wt is the mass of soil in kg used for the reaction.

Light fraction (LF) material was isolated from the soil samples using a modified version of the method described by Janzen et al. (1992). Specifically, 10 g of soil was weighed and added to 40 mL NaI with a density of 1.7 g $cm^{-3}$. The tubes were shaken, and then allowed to settle for 48 h before floating material was removed, and the remaining

**Table 2**
Absorption bands in the mid-infrared used to evaluate FTIR spectra of soil. Assignment based on Calderón et al., 2013 and Parikh et al., 2014.

| Wavenumber ($cm^{-1}$) | Assignment |
|---|---|
| 3620 | Stretching O–H in clays |
| 3200–3500 | O–H, N–H stretch |
| 2934 | Aliphatic C–H stretch |
| 2859 | Aliphatic C–H stretch |
| 2110 | Carbohydrates overtones of the–COH stretch |
| 1790–2000 | Silicates Si-O stretching |
| 1730–1700 | C = O ester stretching |
| 1635–1680 | Amide I: C = O, C–N, N–H |
| 1580–1600 | Aromatic C = C stretch |
| 1575 | Amide II: N–H, C–N |
| 1471–1426 | C–H and N/H amide II, aliphatic C–H deformation |
| 1405 | Aliphatic C–H |
| 1390 | Aliphatic, symmetric C–H bending |
| 1270 | Phenol $CH_2$ deformation, C-O of phenolic OH |
| 1170 | Aliphatic, O–H, C-OH stretch |
| 1000–1100 | Silicates Si-O stretching |
| 1080 | Polysaccharides C–C stretch, C–O stretch |
| 1016 | Polysaccharide C-O-C, C-OH stretch |

substance was filtered using a fiberglass filter in a Buchner funnel. The dried organic material was separated from the surface of the filter paper with a brush before being weighed.

### 2.6. Infrared spectroscopy Fourier transform mid-infrared spectroscopy (FTIR)

Whole soils and LF material were air-dried, ground, and scanned undiluted (neat) on the mid-infrared spectrometer from 4000 to 400 $cm^{-1}$. Two FTIR spectra per sampling site (a single spectrum per replicate) were recorded using a Digilab FTS 7000 spectrometer (Agilent Technologies, Walnut Creek, CA) with a KBr beam splitter, and a Peltier-cooled DTGS detector. Subsequently, a representative and average normalized spectrum over the different sites was calculated. The samples were analyzed in diffuse reflectance, at 4 $cm^{-1}$ resolution, and each spectrum consisted of 64 co-added scans. The dominant functional groups in the FTIR spectra obtained from whole soils and LF are further described in Table 2.

### 2.7. Statistical analyses

Data was checked for a normal distribution using the Shapiro-Wilk normality test. If necessary, data were square root or log transformed to approximate normality. If the normality assumptions were not satisfied, non-parametric statistical tests were used. Correlations between soil properties and climate variables were conducted using non-parametric Spearman's rank correlation coefficient in Sigma Plot 13.0 (Systat Software, San Jose, California). Data among treatments were explored with one-way ANOVA (critical P value 0.05) followed by a multiple range test was achieved using the least significant difference (LSD, $p < 0.05$) in Statgraphics plus 5.1 (Manugistics, Inc., Rockville, MD, USA). A two-way ANOVA as a function of two factors: (1) climate and (2) land use, as independent sources of variance, was performed to test the interaction with labile organic fractions (SOC, POXC, POXC/SOC, LF, and WSA).

A canonical redundancy analysis (RDA) was conducted to identify relationships between environmental variables and spectral data. The analysis was performed using Canoco software v5.0 (Microcomputer Power, USA). Redundancy analysis is a constrained version of PCA which summarizes linear relationships between response variables that are explained by explanatory variables. RDA were performed by using all variables shown in Table 1. This can potentially introduce some overfitting but including all response variables and environmental factors was deemed beneficial in order to illustrate a more inclusive set of relationships. In addition, following the RDA, a variation partitioning analysis (Borcard et al., 1992) was used to quantify the independent or overlapping effects of explanatory variables (climate and land use) on SOC fractions.

The Unscrambler 10.3 software package (CAMO, Norway) was used to perform principal components analyses (PCA) on the mid-infrared spectral data. The average whole soil and LF spectra were baseline corrected using the baseline offset feature in Unscrambler 10.3 (Camo Software, Norway) before being used in the RDA analysis. Spectral bands were selected from the average whole soil and LF spectra using the peak picking feature in ThermoGRAMS software (Thermo Fischer Scientific Inc., Massachussetts, USA). The absorbance data was mean centered, and a PCA of whole soil and LF mid-infrared spectra was performed using Unscrambler 10.3 software (Camo Software, Norway). Component loadings were used to determine the contribution of spectral bands to the variation in soil total organic C and to the variation in POXC content.

## 3. Results and discussion

### 3.1. FTIR analysis in LF

The spectra obtained directly from the LF material, differ greatly from those of the whole soil (Fig. 2). LF content is prone to rapid mineralization due to the labile nature of its constituents and the lack of protection by soil colloids (Turchenek and Oades, 1979), which is consistent with the absence of mineral spectral bands from clays at 3620 $cm^{-1}$ and silicates at 1875 $cm^{-1}$ observed in this study. Overall, several organic spectral bands were enhanced in the LF spectra. For example, the broad band at 3500–3200 $cm^{-1}$ was much more pronounced compared to the whole soil spectra. This band is associated with OH or NH stretching, typical of fresh crop residues (Parikh et al., 2014). The band between 2930 and 2850 $cm^{-1}$, attributed to aliphatic CH stretching, were also more marked in LF spectra than in whole soil spectra. The bands observed from 1700 $cm^{-1}$ to 1250 $cm^{-1}$ contain information about several functional groups such as esters (1730 to 1700 $cm^{-1}$) and carboxylic acids. Calderón et al. (2011) found similar results in a diverse soil collection from the North American Midwest, where LF was distinguishable from heavier fractions because of high absorbance at 3400 $cm^{-1}$ (OH/NH), as well as between 1750 and 1350 $cm^{-1}$. As the soil undergoes net C mineralization, the mid-infrared absorbance of LF declines at 3400 $cm^{-1}$, and between 2920 and 2860 $cm^{-1}$, indicating that these could be regarded as labile moieties in LF (Calderón et al., 2011).

Furthermore, the gross chemical behavior of LF generally featured common spectral features, but with different band intensities (Fig. 2a). For instance, the bands at 3400 $cm^{-1}$ and 1660 $cm^{-1}$, attributed to stretching vibration O–H from water, alcohols, carboxylic acids, phenols, and N–H from amides, were more prominent in the spectra of arid soils. It is likely that the chemical composition of plant litter has an influence on spectral changes. However, because LF characteristics were broadly similar even under different vegetation types, we suspect that LF composition seems to depend primarily on other factors than plant litter quality, such as climate conditions which impact plant productivity and decomposition rates. This is consistent with previous studies (Gosling et al., 2013; Rumpel et al., 2012; Song et al., 2012), which support the notion that the processes involved in the formation of LF might be similar and related greatly to climate conditions.

Although it is assumed that light fraction is highly sensitive to changes in management practices (Gregorich and Janzen, 1996; Tan et al., 2007), the response of LF to different climates indicate that warming and increased precipitation may influence certain fractions of soil organic matter (Song et al., 2012). Our results showed a significant negative effect ($p < 0.05$) of MAT on LF content ($r = -0.72$) (Table 3); however, no significant relationship was found between LF content and precipitation. To test the influence of edaphic and climatic

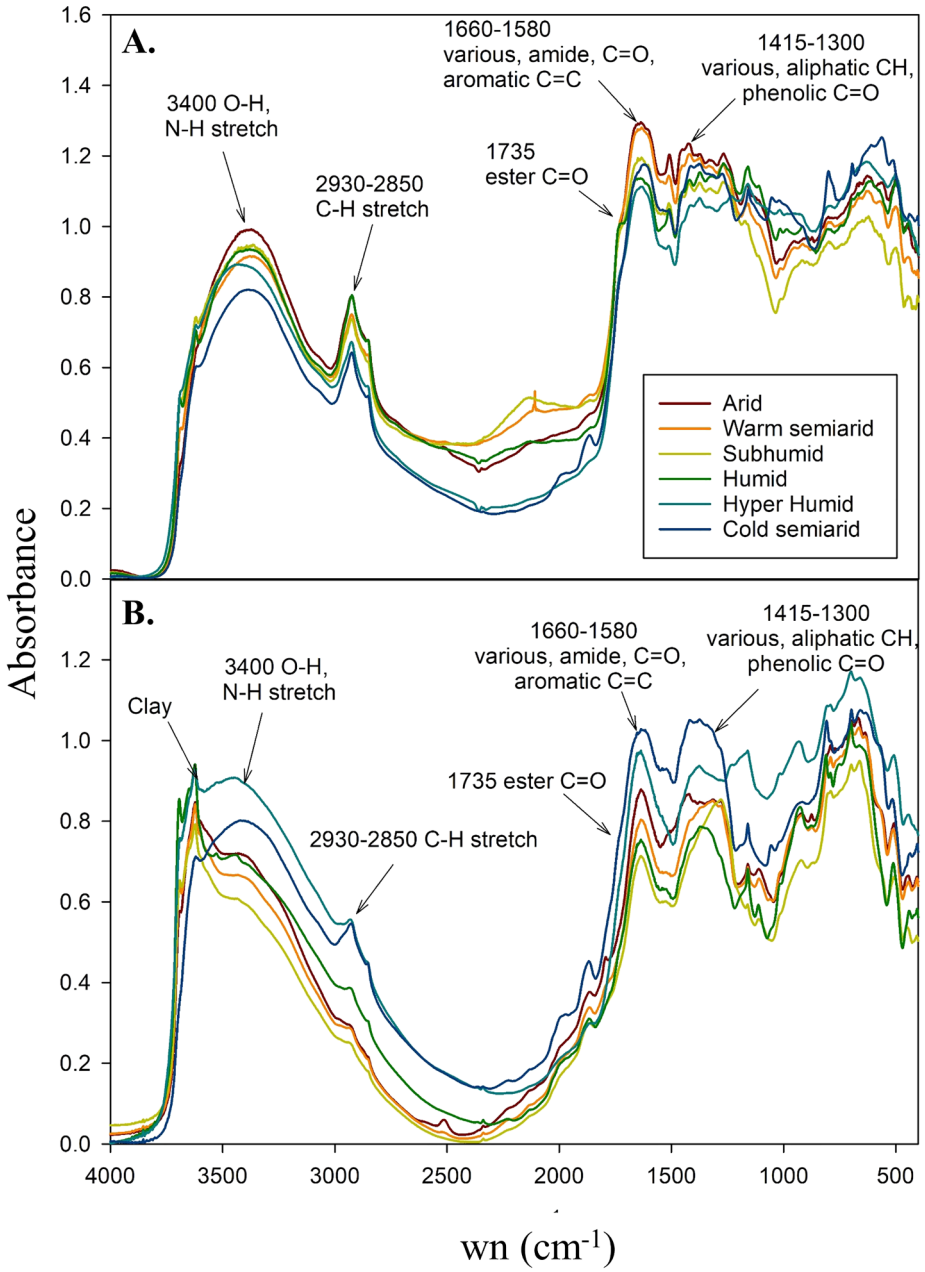


**Fig. 2.** Average Fourier transform mid-infrared spectra for each aridity class. A) Light fraction material, and B) whole soil spectra. Absorbances were baseline corrected using the baseline offset feature in Unscrambler 10.3 (Camo Software, Norway) in order to achieve a common low absorbance for all the averages.

**Table 3**
Spearman's rank correlation coefficient among soil and climates attributes used in the study.

| | LF | SOC | POXC/SOC | WSA | MAP | MAT | Sand | Silt | Clay | C:N | pH |
|---|---|---|---|---|---|---|---|---|---|---|---|
| POXC | 0.72* | 0.80* | −0.47* | 0.33* | 0.26* | −0.51* | −0.14 | 0.40* | −0.25* | −0.30* | −0.25* |
| LF | | 0.70* | −0.51* | 0.38* | 0.19 | −0.72* | 0.04 | 0.37* | −0.44* | −0.39* | −0.36* |
| SOC | | | −0.88* | 0.69* | 0.60* | −0.73* | −0.11 | 0.38* | −0.28* | −0.32* | −0.65* |
| POXC/SOC | | | | −0.79* | −0.74* | 0.66* | −0.01 | −0.21 | 0.31* | 0.26* | 0.78* |
| WSA | | | | | 0.55* | −0.66* | 0.11 | 0.04 | −0.28* | −0.39* | −0.75* |
| MAP | | | | | | −0.47* | −0.02 | 0.11 | −0.16 | 0.03 | −0.72* |
| MAT | | | | | | | −0.08 | −0.30* | 0.45* | 0.46* | 0.61* |
| Sand | | | | | | | | −0.70* | −0.72* | −0.09 | −0.07 |
| Silt | | | | | | | | | 0.08 | −0.09 | −0.11 |
| Clay | | | | | | | | | | 0.22 | 0.26* |
| C:N | | | | | | | | | | | 0.21 |

(*) There is significant relationship between two variables ($P < 0.05$).
MAT: mean annual temperature (°C); MAP: mean annual precipitation (mm/yr$^{-1}$); LF: light fraction (g kg$^{-1}$); POXC: permanganate oxidizable carbon (g kg$^{-1}$); SOC: soil organic carbon (%); WSA: water stable aggregates.

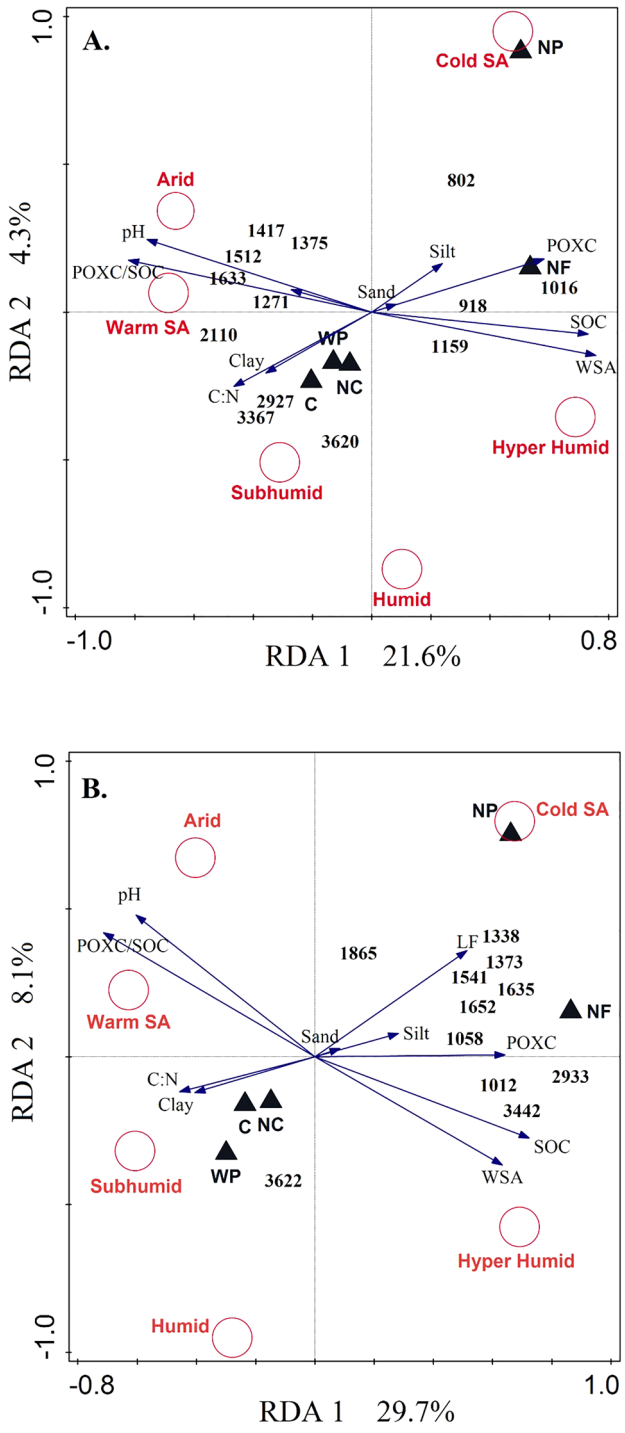


**Fig. 3.** Redundancy analysis (RDA) showing the relationships between FTIR bands, SOC labile fractions (POXC and LF), and soil properties and environmental factors including aridity regime and land use. WP: Woody perennial; C: Cultivated; NC: Non-cultivated; N: Natural prairie, NF: Native forest. A) Light fraction material, and B) whole soils.

factors on the composition of LF, an RDA analysis was carried out with FTIR functional groups (Fig. 2a). Comparing the effect of different climates regimes, we observed that climates played a vital role in the labile C pools decomposition. Along the first axis, which explains 21.6% of the total variance (Fig. 3a), the spectral bands were clearly clustered according to climate regime. LF spectra from arid, warm semiarid, and subhumid soils, with high POCX/SOC had high absorbance at multiple organic bands. These included 2110 (overtones of the–COH stretch), 3367 (O–H, N–H stretch), 2927 (aliphatic C–H stretch) and 1633 $cm^{-1}$ (amide 1). In addition, the results revealed the prevalence of relatively chemically complex LF material in low SOC soils. For instance, absorbances at 1512 $cm^{-1}$ and 1633 $cm^{-1}$, possibly due to lignin derivatives, were more pronounced under arid/warmer conditions, and defined band maxima at 2927 $cm^{-1}$ at 3367 $cm^{-1}$ were observed in soils from subhumid regions. These bands can be assigned to O–H and N–H stretch, aliphatic CH, amide I, and aromatic C = C, respectively. LF composition is characterized by the presence of carbohydrates and aliphatic substances, which play important roles in the chemical composition of this fraction (Golchin et al., 1994). Thus, absorbance at 1016 $cm^{-1}$, attributed to polysaccharide C-O-C, C-OH stretch (Parikh et al., 2014), was higher in soils with high SOC and soil aggregation, mostly from colder climates (Fig. 3a). The polysaccharide accumulation possibly resulted from the effects of temperature on the microbial transformation rate of raw material into more decomposition-resistant molecules. Such patterns, are consistent with Morrison et al. (2019), who found that the chemistry of leaf litter from two years heated soils had a greater relative abundance of lignin, while the relative abundance of more labile compounds like plant lipids and polysaccharides was low.

### 3.2. FTIR analysis of whole soils

The results showed that whole soil spectra contained absorbance bands attributable to mineral and organic matter. The arid whole soil spectrum featured absorbance bands at 1870 $cm^{-1}$ attributed to Si-O bonds, which is characteristic of quartz and sands, and 3620 $cm^{-1}$ associated with hydroxyl stretching of clay minerals, as well as a relatively weak band at 2510 $cm^{-1}$ representing carbonates that was absent on the spectra of all other aridity regimes (Fig. 2b). This fits with other studies that have suggested that arid and semiarid areas in Chile frequently contain calcareous alkaline soils (Casanova et al., 2013). There was a tendency for specific regions of the spectrum to become more intense for whole soil samples from cold and humid areas, which may indicate less degradation of organic matter compared to warmer areas and layers of silicates. More specifically, the band residing at 3400 $cm^{-1}$ and a single broad band at 1030–1010 $cm^{-1}$ attributed to Si–O stretching were particularly pronounced in soils from cold semiarid and hyper humid climates, which are also characterized by high SOC content (Fig. 2b).

The RDA analysis for whole soils, in which the first axis explained 29.7% and the second axis 8.1% of the total variance, shows that the MidIR absorbance data contained several spectral bands that were related to specific soil properties (Fig. 3b). For instance, as expected, sand content was positively correlated with absorbances at 1865 $cm^{-1}$, corresponding to silicate Si-O absorbance. Soils from cooler (cold semiarid, hyper humid, humid) and warmer (warm semiarid, arid, and subhumid) climates were separated into two groups according to pH, POXC/SOC, and spectral properties (Fig. 3b). Aromatic structures declined under warmer climates, and there was aliphatic enrichment in soils higher in SOC and POXC content, mostly soils from hyper humid sites. Higher absorbances for C-O stretching of polysaccharides around 1012–1058 $cm^{-1}$ and OH/NH functional groups at 3442 $cm^{-1}$ were observed for colder climates. Polysaccharide accumulation possibly resulted of bridging role of polysaccharides with mineral surfaces, which contribute to formation and stabilization of stable aggregates (Kiem and Kögel-Knabner, 2003; Oades, 1984; Srivastava et al., 2019). In addition, previous studies have shown that soils high in POXC contain increased proportions of aliphatic chemical species (Calderón et al., 2017; Margenot et al., 2015; Romero et al., 2018). The aliphatic component of SOM may frequently come from either inputs of aliphatic-rich OM or through production of aliphatic compounds from microbial decomposition (Baddi et al., 2004; Hsu and Lo, 1999).

### 3.3. Linking organic matter stabilization to labile SOC fractions

Stabilization of SOM often includes physical mechanisms, such as aggregation or sorption, chemical protection, and perturbations, such as N enrichment, that serve to accelerate or inhibit the activity of some enzymes or microbial groups (Grandy and Neff, 2008; Lützow et al., 2006). On a country-wide scale, SOC was positively correlated ($p < 0.05$) with both POXC ($r = 0.80$), LF ($r = 0.70$) and WSA ($r = 0.69$). In Addition, there was a significant effect of WSA on the concentrations POXC ($r = 0.33$) and LF content ($r = 0.38$) (Table 3). Along with POXC and LF in whole soil spectra (Fig. 3b), soil aggregation also correlated positively with aliphatic components and the band at 1635 $cm^{-1}$ corresponding to amide or ketone C = O (Figs. 2b and 3b), whereas soils with low aggregation, mainly those from warmer climates, did not correlated with any band (Fig. 3b). These results indicate that MidIR data has certain chemical moieties that are more prevalent in samples with good soil quality attributes. Consistent with these findings, a recent study by Sarker et al. (2018) showed that structures such as O-alkyl and di-O-alkyl are positively associated with aggregate stability and soil structure, whereas aromatic C fractions are negatively correlated with soil aggregation, possibly due to aggregates being protected by coatings associated with water repellency.

Negatively charged clay minerals promote sorption of organic groups contributing to SOM stabilization (Wiesmeier et al., 2019). An inverse relationship ($p < 0.05$) was found between clay and POXC ($r = -0.25$) as well as between clay and LF ($r = -0.44$) (Table 3). Furthermore, clay and POXC/SOC were positively correlated ($r = 0.31$), however, these relationships differed when clay and the proportion of POXC to SOC content (POXC/SOC) were analyzed separately ($p < 0.05$) for warmer areas ($r = -0.46$) and for colder areas ($r = 0.35$). This may indicate the functional relevance of clay minerals in the formation of stable soil C through chemical binding of newer and less chemically complex compounds in warmer areas (Bach et al., 2018; Jones and Donnelly, 2004; Post and Kwon, 2000). In addition, negative relationships ($p < 0.05$) were also observed between C:N and POXC ($r = -0.30$) and between C:N and SOC ($r = -0.32$) (Table 3). These inverse trends are consistent with previous results observed for other labile or active fractions strongly associated with POXC, such as soil microbial biomass (Wardle, 1992). Previous studies have demonstrated that soil C:N ratio is an important factor in controlling microbial communities (Chu et al., 2010; Shen et al., 2013), indicating that in many soil ecosystems soil N rather than soil C may influence the immobilization of SOM by microbial biomass (Wiesmeier et al., 2019).

### 3.4. Spectral changes associated with SOC and POXC

In addition to the RDA analysis, PCA was conducted in order to identify the spectral regions explaining the major spectral differences in LF spectra (Fig. 4) and in whole soil spectra (Fig. 5) with respect to SOC and POXC content. Overall, the spectral features of LF in cooler SOC-rich soils tended to be closer, when compared to LF with lower SOC content ranging between 0.6 and 3.2%, mostly found in warmer areas

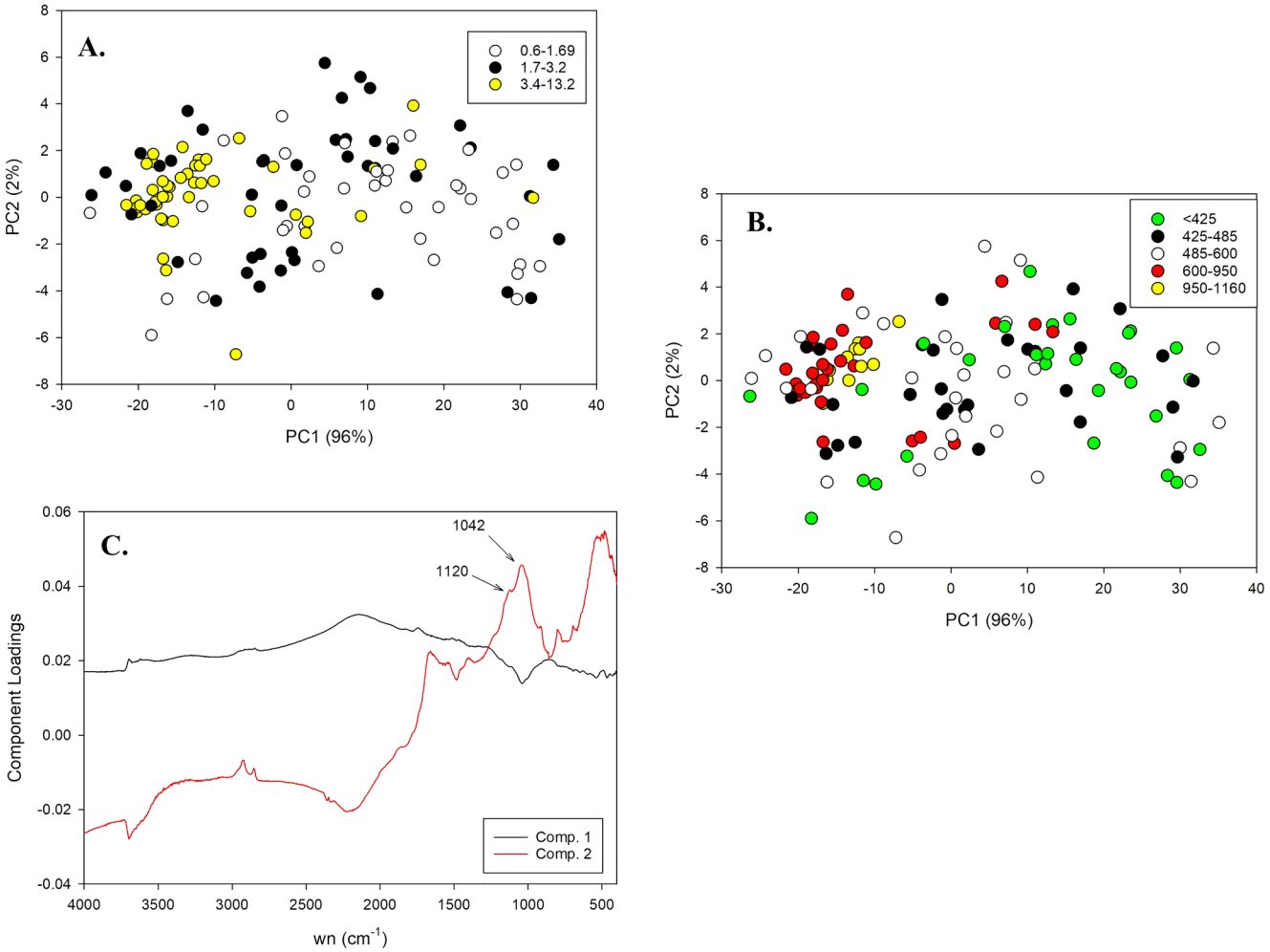


**Fig. 4.** Principal components analysis (PCA) of the mid-infrared spectral data for light fraction (LF). Color coded according to (A) soil total organic C (%), and (B) POXC content (mg $kg^{-1}$). The component loadings for the PCA are shown in (C).

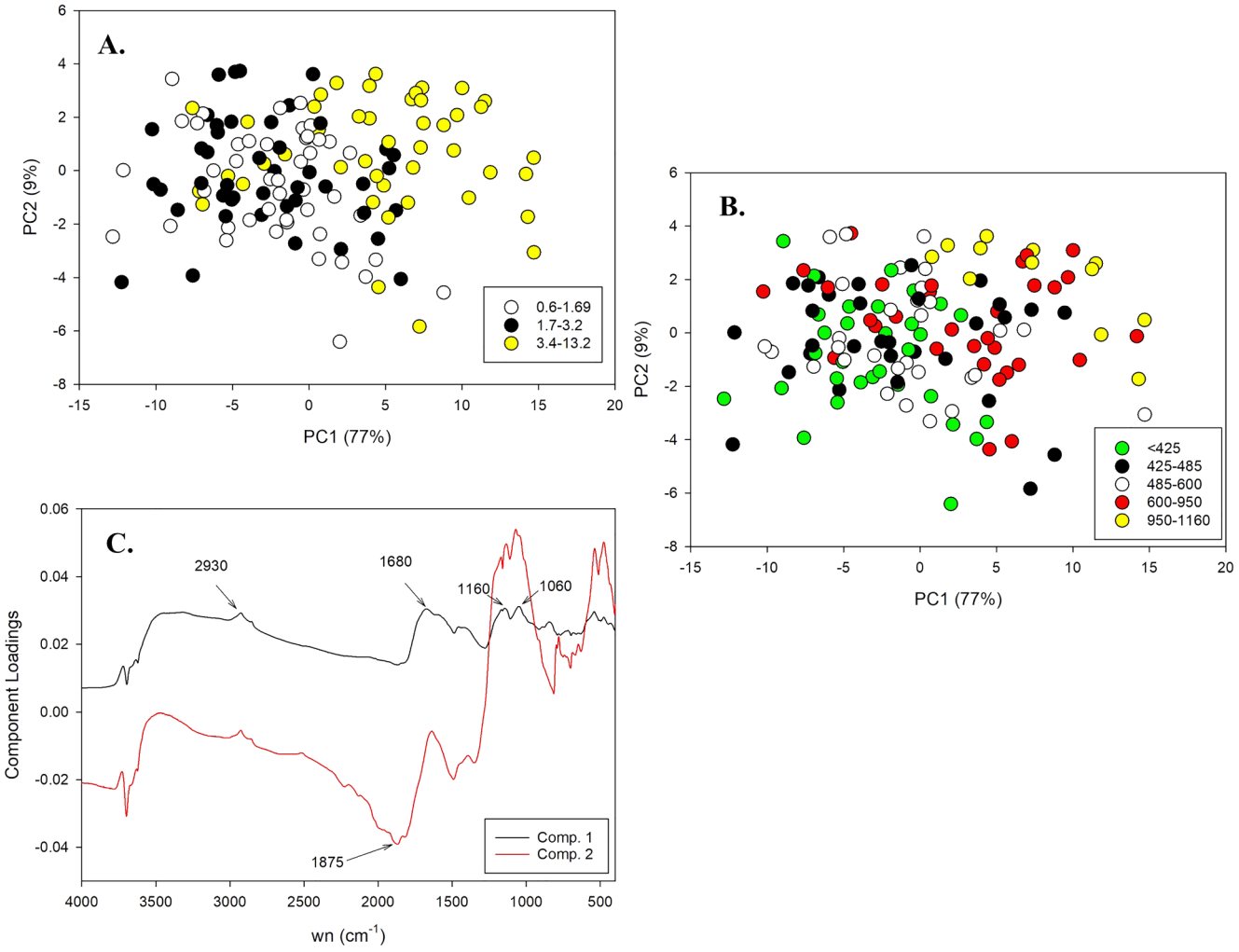


**Fig. 5.** Principal components analysis (PCA) of the mid-infrared spectral data for whole soils. Color coded according to (A) soil total organic C (%), and (B) POXC content (mg $kg^{-1}$). The component loadings for the PCA are shown in (C).

(Fig. 4a). A similar pattern was found in the relationship between POXC and LF spectra (Fig. 4b). For whole soils spectra, the bands tended to cluster together in a one group and were more clearly defined in relation to SOC content (i.e. samples with increasing SOC and POXC tended towards the right of the PCA plane) (Fig. 5a and b). While SOM content does not seem to vary in relation to spectral characteristics of LF composition (i.e. the separation of data clusters is not so clearly defined), SOM content in whole soil responded to bands or regions that share similar spectral characteristics. Such findings suggest that, whereas SOC accumulation would not be primarily associated with the chemical composition of LF materials, the spectral chemical composition of whole soils seem to be related to SOC content. Our results might

**Table 4**
Mean values and standard deviations for soil total organic carbon (SOC), permanganate oxidizable carbon (POXC), and LF (light fraction) categorized according to aridity regime and land use type of the 74 soils studied.

| | SOC ($g\ kg^{-1}$) | POXC ($mg\ kg^{-1}$) | POXC/SOC (%) | LF ($g\ kg^{-1}$) | WSA (% > 0.25 mm) |
|---|---|---|---|---|---|
| Aridity regime[a] | | | | | |
| Arid | 14.9 ± 4.6a | 457 ± 95a | 3.2 ± 0.3a | 9.0 ± 2.4a | 64.2 ± 8.9ab |
| Warm semiarid | 15.7 ± 6.9a | 470 ± 161a | 3.2 ± 0.8a | 9.6 ± 8.5a | 64.1 ± 11.8a |
| Subhumid | 17.4 ± 7.5a | 439 ± 143a | 2.6 ± 0.3a | 3.9 ± 1.1a | 75.1 ± 8.1b |
| Humid | 29.2 ± 7.0ab | 424 ± 79a | 1.5 ± 0.2bc | 10.0 ± 4.3a | 89.5 ± 7.8c |
| Hyperhumid | 77.7 ± 36.5c | 796 ± 256b | 1.2 ± 0.3c | 38.2 ± 40.8a | 89.2 ± 4.1c |
| Cold semiarid | 44.7 ± 14.9b | 727 ± 188b | 1.8 ± 0.5b | 108.0 ± 101.5b | 86.9 ± 9.0c |
| Land use | | | | | |
| Native forest | 66.8 ± 33.5b | 806 ± 186a | 1.4 ± 0.5a | 70.1 ± 51.8ab | 82.3 ± 12.6ab |
| Natural prairie | 44.9 ± 16.2ab | 700 ± 192a | 1.7 ± 0.5a | 113.2 ± 110.8a | 89.4 ± 5.5b |
| Non-cultivated | 38.0 ± 36.4ab | 611 ± 241ab | 2.4 ± 1.1ab | 20.0 ± 28.3bc | 75.4 ± 17.8a |
| Cultivated | 30.9 ± 29.5a | 518 ± 213b | 2.4 ± 1.1b | 12.1 ± 12.8c | 74.5 ± 14.3a |
| Woody perennial | 33.2 ± 32.7ab | 499 ± 270b | 2.1 ± 0.8ab | 14.1 ± 13.3bc | 79.1 ± 9.7ab |

Different letters within each column indicate significant differences between treatments at $P < 0.05$.
[a] Aridity regime, defined by the aridity index based on UNEP (1992) and UNESCO (2010).

support the fact that specific ecosystem property such as geographic variation, climate, physical protection and mineralogical composition appear to have an important role in the persistence and accumulation of SOC (e.g. Al-rich allophanic Andisols) (Matus et al., 2006; Schmidt et al., 2011; Wiesmeier et al., 2019).

The loading of component 1 (PC1) for LF spectra (Fig. 4c), explaining 92% of the variance, shows that spectral differences were associated with higher absorbances in the 1042 $cm^{-1}$–1120 $cm^{-1}$ region, which can be attributed to C-O stretching of polysaccharides (Fig. 4c). PC1 loadings for whole soils (Fig. 5c), explaining 77% of the variance, the spectral differences were associated with higher absorbances at several bands: 2930, 1680, 1160, and 1060 $cm^{-1}$ corresponding to aliphatic C-H, amide, and C-O stretching of polysaccharides and/or Si-O stretching vibrations near 1100 $cm^{-1}$ region corresponding to phyllosilicates, respectively. It is likely that the composition of Andisols, one the soil types collected, may have contribute strongly with the prevalence of these absorption bands. Andisols are characterized by a high aggregate stability as well high concentrations of SOC, mainly associated with their mineralogical composition. Thus, amorphous inorganic materials, such as smaller or less-crystalline phyllosilicate contribute to increasing aggregation and organic matter stabilization (Asano and Wagai, 2014; Matus et al., 2014). The loading of component 2 (PC2) that accounted for 9% variance for whole soils (Fig. 5c), showed a negative correlation with bands corresponding to silicate (Si-O) and clay minerals at 1875 $cm^{-1}$ and 3620 $cm^{-1}$, respectively. The negative correlation of PC2 with the band related to clay is consistent with the low clay content observed in soil SOC-rich soils samples (Table 1). This suggest that as such variations in the spectral composition do occur, clay minerals do not seem to affect SOC stabilization in soil with high levels of SOC. However, at low carbon contents, it seems that mineral absorption bands due to structural OH and Si–O groups may have an important role in C accumulation, which might be involved in sorption of SOC to phyllosilicate clay, thus contributing to preservation of SOC in warmer areas.

### 3.5. Linking climate and land use to labile SOC fractions

In this study, the variability of POXC and LF was examined across a set of climates and land use types in Chile. POXC content was significantly higher ($p < 0.05$) in cold semiarid and in hyper humid conditions than in arid/warmer climates (Table 4). Moreover, permanganate oxidizable C was strongly correlated with SOC in all the 75 sites studied (Fig. 6). The line of best fit between SOC and POXC was hyperbolic rather than linear ($R^2 = 0.69$; Fig. 6). These observations are in agreement with previous studies (Bongiorno et al., 2019; Duval et al., 2018), which suggest that POXC represents the labile fraction most strongly related to SOC and particularly sensitive to climate variations. In addition, the proportion of POXC in SOC (POXC/SOC) decreased when climate became more humid and cooler, ranging from 3.2% in soils from arid-semiarid climates to just 1.2% in hyper humid soils. SOM decomposition is strongly accelerated by warm conditions, which result in a decrease in SOC that is in turn ended in a high POXC/SOC ratio (Allison et al., 2010; Culman et al., 2012). Alternatively, POXC has also been considered a more processed or stabilized pool that lead to organic matter formation (Hurisso et al., 2016; Tirol-Padre and Ladha, 2004). Therefore, the transformation of POXC into SOM might occur at a slower rate under warmer conditions, increasing the POXC level relative to SOC.

In order to determine how the variation in soil chemical composition influences POXC under different climate conditions, two correlation analyses between POXC and MidIR absorbances were carried out: one was performed using whole soils from cooler climate regimes, which typically have high levels of SOC, and the other one was performed using whole soils under warmer climates (Fig. 7). These results suggest that POXC was strongly negatively correlated with clay absorbance bands at 3630–3700 $cm^{-1}$ in soils from warm climates, likely

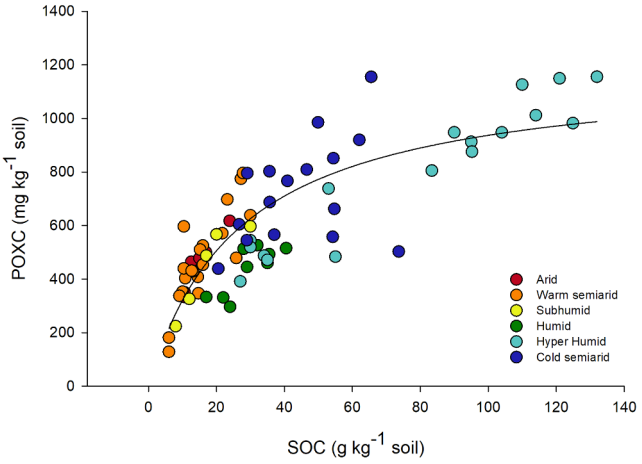


**Fig. 6.** Hyperbolic fit lines for soil organic carbon (SOC) vs. permanganate oxidizable carbon (POXC). Red symbols are arid sites, orange symbols are warm semiarid sites, blue symbols are cold semiarid sites, green symbols are humid sites, light blue symbols are humid sites, and blue symbols are cold semiarid sites.

indicating that the accumulation of alkyl C in soils is favored by the presence of clay mineral surfaces. In addition, a different set of spectral bands were positively correlated with POXC for warmer climate. These were the aliphatic CH band at 2930–2850 $cm^{-1}$, and a broad band at 1190 $cm^{-1}$ corresponding to polysaccharide. For SOC-rich cold soils, absorbances at 3450–2820 and 1730–1000 $cm^{-1}$ were positively correlated with POXC. These spectral regions contain many of the bands associated with a variety of organic moieties (Parikh et al., 2014).

We were not able to find any pure dependence on land use for POXC, and POXC/SOC, however, climate accounted for at least 26% of the total variance for these variables (Table 5). Similarly, there were no pure effects of land use type on LF, however, a greater proportion of variability was accounted for by both climate and land use (34.8%) in this fraction. Although, significant differences in LF ($p < 0.05$) were observed between agricultural land and undisturbed conditions (natural prairie and native forest) (Table 4), the absence of pure effects of land use on both LF and POXC distinguish the role of climate when soil management is studied under regional-scale conditions. In addition, the remaining variation in SOC fractions, which cannot be attributed uniquely to either explanatory dataset, may be explained by others factor

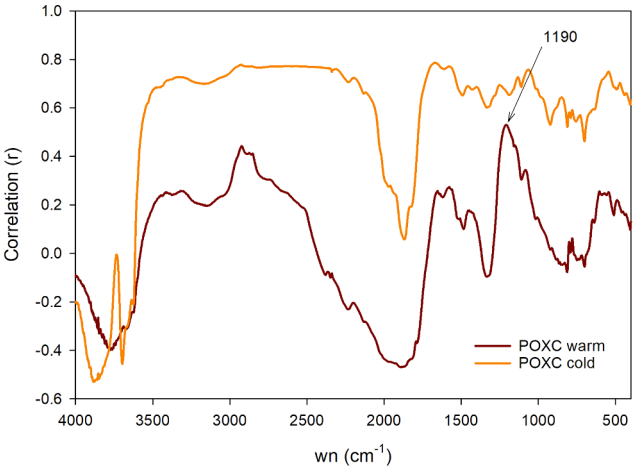


**Fig. 7.** Correlation (r) between whole soil absorbance and POXC. The warm correlation refers to soils from the semiarid, arid, and subhumid sites (n = 68). The cold correlation refers to soils from the cold semiarid, humid, and hyper humid sites (n = 69).

**Table 5**
Two-way ANOVA of the effects of climate and land use on organic fractions, and variation partitioning analysis of organic fractions explained by climate, land use, and shared effects.

| Organic Fractions | Two-way ANOVA | | Variation explained (%) | | |
|---|---|---|---|---|---|
| | Climate | Land use | Climate | Land use | Share effects |
| SOC | *** | ns | 55.5 | 0.5 | 3.6 |
| POXC | *** | ns | 26.5 | 0 | 11.7 |
| POXC/SOC | *** | ns | 62.9 | 0 | 6.5 |
| LF | ns | ns | 0 | 0 | 34.8 |
| WSA | *** | ns | 52.7 | 3.0 | 7.2 |

*** Statistically significant difference ($P < 0.001$).
ns: non-significant relationship ($P > 0.05$).
LF: light fraction; POXC: permanganate oxidizable carbon; SOC: soil organic carbon; WSA: Water stable aggregates.

not included in this study such as topography, soil type, vegetation, and management history (Duval et al., 2018; Wiesmeier et al., 2019).

## 4. Conclusions

Under a wide range of climates and land use types, the chemical composition of LF material and whole soil was closely related to aliphatic structures in cooler areas. In contrast, LF contained more chemically complex structures in warmer areas. This indicates that organic rich soils would have slow decomposition rates of plant material as a result of lower temperature as well other properties such as soil aggregation, which accelerate or delay the microbial transformation of raw materials into more decomposition-resistant compounds. The main results suggest that the spectral features of LF material and whole soils are potential indicators for screening early disturbances of soil functioning, however, further studies are needed to evaluate direct effects of their chemical composition on SOC accumulation. POXC was closely related to SOC content and exhibited similar spectral features to the SOC content. POXC might be used as a rapid indicator of soil quality; however, is strongly influenced by climate variability. Such chemical changes presented this study has significant implications on how accumulation of chemically distinct organic compounds have many effects on ecosystem level processes, which may contribute to identifying areas that are more vulnerable to SOC losses.

## Declaration of Competing Interest

The authors declare that they have no known competing financial interests or personal relationships that could have appeared to influence the work reported in this paper.

## Acknowledgments

This research was supported by funding from the National Commission for Scientific and Technological Research, CONICYT/FONDECYT/Regular 1161045. P. Ramírez thanks the support from CONICYT Doctorado Nacional Scholarship 21140873, Government of Chile.

## Disclaimer

The use of trade, firm, or corporation names is for the information and convenience of the reader. Such use does not constitute an official endorsement or approval by the United States Department of Agriculture or the Agricultural Research Service of any product or service to the exclusion of others that may be suitable. The U.S. Department of Agriculture (USDA) prohibits discrimination in all its programs and activities on the basis of race, color, national origin, age, disability, and where applicable, sex, marital status, familial status, parental status, religion, sexual orientation, genetic information, political beliefs, reprisal, or because all or part of an individual's income is derived from any public assistance program.

## References

Allison, S.D., Wallenstein, M.D., Bradford, M.A., 2010. Soil-carbon response to warming dependent on microbial physiology. Nat. Geosci. 3, 336–340. https://doi.org/10.1038/ngeo846.
Asano, M., Wagai, R., 2014. Evidence of aggregate hierarchy at micro- to submicron scales in an allophanic andisol. Geoderma 216, 62–74. https://doi.org/10.1016/j.geoderma.2013.10.005.
Bach, E.M., Williams, R.J., Hargreaves, S.K., Yang, F., Hofmockel, K.S., 2018. Greatest soil microbial diversity found in micro-habitats. Soil Biol. Biochem. 118, 217–226. https://doi.org/10.1016/j.soilbio.2017.12.018.
Baddi, G.A., Alburquerque, J.A., Gonzálvez, J., Cegarra, J., Hafidi, M., 2004. Chemical and spectroscopic analyses of organic matter transformations during composting of olive mill wastes. Int. Biodeterior. Biodegrad. 54, 39–44. https://doi.org/10.1016/j.ibiod.2003.12.004.
Biederbeck, V.O., Janzen, H.H., Campbell, C.A., Zentner, R.P., 1994. Labile soil organic matter as influenced by cropping practices in an arid environment. Soil Biol. Biochem. 26, 1647–1656. https://doi.org/10.1016/0038-0717(94)90317-4.
Blair, G.J., Lefroy, R.D., Lisle, L., 1995. Soil carbon fractions based on their degree of oxidation, and the development of a carbon management index for agricultural systems. Aust. J. Agric. Res. 46, 1459–1466. https://doi.org/10.1071/AR9951459.
Bongiorno, G., Bünemann, E., Oguejiofor, C., Meier, J., Gort, G., Comans, R., Mäder, P., Brussaard, L., de Goede, R., 2019. Sensitivity of labile carbon fractions to tillage and organic matter management and their potential as comprehensive soil quality indicators across pedoclimatic conditions in Europe. Ecol. Indic. 99, 38–50.
Bonilla, C.A., Johnson, O.I., 2012. Soil erodibility mapping and its correlation with soil properties in Central Chile. Geoderma 189–190, 116–123. https://doi.org/10.1016/j.geoderma.2012.05.005.
Bonilla, C.A., Vidal, K.L., 2011. Rainfall erosivity in Central Chile. J. Hydrol. 410, 126–133. https://doi.org/10.1016/j.jhydrol.2011.09.022.
Borcard, D., Legendre, P., Drapeau, P., 1992. Partialling out the spatial component of ecological variation. Ecology 73, 1045–1055. https://doi.org/10.2307/1940179.
Bradford, M.A., Wieder, W.R., Bonan, G.B., Fierer, N., Raymond, P.A., Crowther, T.W., 2016. Managing uncertainty in soil carbon feedbacks to climate change. Nat. Clim. Chang. 6, 751. https://doi.org/10.1038/nclimate3071.
Calderón, F., Haddix, M., Conant, R.T., Magrini-Bair, K., Paul, E., 2013. Diffuse-Reflectance Fourier-Transform Mid-Infrared Spectroscopy as a Method of Characterizing Changes in Soil Organic Matter. Soil Sci. Soc. Am. J. 77, 1591–1600. https://doi.org/10.2136/sssaj2013.04.0131.
Calderón, F.J., Culman, S., Six, J., Franzluebbers, A.J., Schipanski, M., Beniston, J., Grandy, S., Kong, A.Y.Y., 2017. Quantification of Soil Permanganate Oxidizable C (POXC) Using Infrared Spectroscopy. Soil Sci. Soc. Am. J. 81, 277. https://doi.org/10.2136/sssaj2016.07.0216.
Calderón, F.J., Reeves, J.B., Collins, H.P., Paul, E.A., 2011. Chemical Differences in Soil Organic Matter Fractions Determined by Diffuse-Reflectance Mid-Infrared Spectroscopy. Soil Sci. Soc. Am. J. 75, 568. https://doi.org/10.2136/sssaj2009.0375.
Cambardella, C.A., Elliott, E.T., 1992. Particulate Soil Organic-Matter Changes across a Grassland Cultivation Sequence. Soil Sci. Soc. Am. J. 56, 777–783. https://doi.org/10.2136/sssaj1992.03615995005600030017x.
Casanova, M., Salazar, O., Seguel, O., Luzio, W., 2013. The Soils of Chile. World Soil Book Series, Springer, Dordrecht.
Chu, H., Fierer, N., Lauber, C.L., Caporaso, J.G., Knight, R., Grogan, P., 2010. Soil bacterial diversity in the Arctic is not fundamentally different from that found in other biomes. Environ. Microbiol. 12, 2998–3006. https://doi.org/10.1111/j.1462-2920.2010.02277.x.
Comino, F., Aranda, V., García-Ruiz, R., Ayora-Cañada, M.J., Domínguez-Vidal, A., 2018. Infrared spectroscopy as a tool for the assessment of soil biological quality in agricultural soils under contrasting management practices. Ecol. Indic. 87, 117–126. https://doi.org/10.1016/j.ecolind.2017.12.046.
Conteh, A., Blair, G.T., Lefroy, R.D.B., Whitbread, A.M., 1999. Labile organic carbon determined by permanganate oxidation and its relationships to other measurements of soil organic carbon. Humic Substances Environmental Journal. Humic Subst. Environ. J. 1, 3–15.
Culman, S.W., Snapp, S.S., Freeman, M.A., Schipanski, M.E., Beniston, J., Lal, R., Drinkwater, L.E., Franzluebbers, A.J., Glover, J.D., Grandy, A.S., Lee, J., Six, J., Maul, J.E., Mirksy, S.B., Spargo, J.T., Wander, M.M., 2012. Permanganate Oxidizable Carbon Reflects a Processed Soil Fraction that is Sensitive to Management. Soil Sci. Soc. Am. J. 76, 494–504. https://doi.org/10.2136/sssaj2011.0286.
Denef, K., Zotarelli, L., Boddey, R.M., Six, J., 2007. Microaggregate-associated carbon as a diagnostic fraction for management-induced changes in soil organic carbon in two Oxisols. Soil Biol. Biochem. 39, 1165–1172. https://doi.org/10.1016/j.soilbio.2006.12.024.
Dimassi, B., Mary, B., Wylleman, R., Labreuche, J., Couture, D., Piraux, F., Cohan, J.P., 2014. Long-term effect of contrasted tillage and crop management on soil carbon dynamics during 41 years. Agric. Ecosyst. Environ. 188, 134–146. https://doi.org/10.1016/j.agee.2014.02.014.
Duval, M.E., Galantini, J.A., Martínez, J.M., Limbozzi, F., 2018. Labile soil organic carbon for assessing soil quality: influence of management practices and edaphic conditions. Catena 171, 316–326.

Gee, G.W., Bauder, J., 1986. Particle-size Analysis. In: Methods of Soil Analysis Part 1. Physical and Mineralogical Methods. Soil Science Society of America. American Society of Agronomy, pp. 383–411.
Golchin, A., Oades, J.M., Skjemstad, J.O., Clarke, P., 1994. Study of free and occluded particulate organic matter in soils by solid state 13C CP/MAS NMR spectroscopy and scanning electron microscopy. Soil Res. 32, 285–309.
Gosling, P., Parsons, N., Bending, G.D., 2013. What are the primary factors controlling the light fraction and particulate soil organic matter content of agricultural soils? Biol. Fertil. Soils 49, 1001–1014. https://doi.org/10.1007/s00374-013-0791-9.
Grandy, A.S., Neff, J.C., 2008. Molecular C dynamics downstream: The biochemical decomposition sequence and its impact on soil organic matter structure and function. Sci. Total Environ. 404, 297–307. https://doi.org/10.1016/j.scitotenv.2007.11.013.
Gregorich, E.G., Ellert, B.H., 1993. Chapter 39: Light Fraction and Macroorganic Matter in Mineral Soils, in: Soil Sampling and Methods of Analysis. pp. 397–407.
Gregorich, E.G., Janzen, H.H., 1996. Storage of soil carbon in the light fraction and macroorganic matter. Struct. Org. Matter Storage Agric. Soils 167–190.
Gregorich, E.G., Monreal, C.M., Carter, M.R., Angers, D.A., Ellert, B.H., 1994. Towards a minimum data set to assess soil organic matter quality in agricultural soils. Can. J. Soil Sci. 74, 367–385. https://doi.org/10.4141/cjss94-051.
Grüneberg, E., Schöning, I., Kalko, E.K.V., Weisser, W.W., 2010. Regional organic carbon stock variability: a comparison between depth increments and soil horizons. Geoderma 155, 426–433. https://doi.org/10.1016/j.geoderma.2010.01.002.
Haynes, R.J., 2005. Labile organic matter fractions as central components of the quality of agricultural soils: an overview. Adv. Agron. 85, 221–268. https://doi.org/10.1016/S0065-2113(04)85005-3.
Hermle, S., Anken, T., Leifeld, J., Weisskopf, P., 2008. The effect of the tillage system on soil organic carbon content under moist, cold-temperate conditions. Soil Tillage Res. 98, 94–105. https://doi.org/10.1016/j.still.2007.10.010.
Hsu, J.H., Lo, S.L., 1999. Chemical and spectroscopic analysis of organic matter transformations during composting of pig manure. Environ. Pollut. 104, 189–196. https://doi.org/10.1016/S0269-7491(98)00193-6.
Hurisso, T.T., Culman, S.W., Horwath, W.R., Wade, J., Cass, D., Beniston, J.W., Bowles, T.M., Grandy, A.S., Franzluebbers, A.J., Schipanski, M.E., Lucas, S.T., Ugarte, C.M., 2016. Comparison of permanganate-oxidizable carbon and mineralizable carbon for assessment of organic matter stabilization and mineralization. Soil Sci. Soc. Am. J. 80, 1352–1364. https://doi.org/10.2136/sssaj2016.04.0106.
Janzen, H.H., Campbell, C.A., Brandt, S.A., Lafond, G.P., Townley-Smith, L., 1992. Light-fraction organic matter in soils from long-term crop rotations. Soil Sci. Soc. Am. J. 56, 1799–1806. https://doi.org/10.2136/sssaj1992.03615995005600060025x.
Jones, M.B., Donnelly, A., 2004. Carbon sequestration in temperate grassland ecosystems and the influence of management, climate and elevated CO2. New Phytol. 164, 423–439. https://doi.org/10.1111/j.1469-8137.2004.01201.x.
Kemper, W.D., Rosenau, R.C., 1986. Aggregate stability and size distribution. methods soil anal. Part 1. Phys. Mineral. methods 9, 425–442. https://doi.org/10.2136/sssabookser5.1.2ed.c17.
Kiem, R., Kögel-Knabner, I., 2003. Contribution of lignin and polysaccharides to the refractory carbon pool in C-depleted arable soils. Soil Biol. Biochem. 35, 101–118. https://doi.org/10.1016/S0038-0717(02)00242-0.
Lal, R., 2016. Soil health and carbon management. Food Energy Secur. 5, 212–222. https://doi.org/10.1002/fes3.96.
Lal, R., 2004. Soil carbon sequestration to mitigate climate change. Geoderma 123, 1–22. https://doi.org/10.1016/j.geoderma.2004.01.032.
Lefèvre, C., Rekik, F., Alcantara, V., Wiese, L., 2017. Soil Organic Carbon the Hidden Potential. Food and Agriculture Organization of the United Nations (FAO). https://doi.org/10.1038/nrg2350.
Leifeld, J., 2006. Application of diffuse reflectance FT-IR spectroscopy and partial least-squares regression to predict NMR properties of soil organic matter. Eur. J. Soil Sci. 57, 846–857. https://doi.org/10.1111/j.1365-2389.2005.00776.x.
Lobo, G.P., Frankenberger, J.R., Flanagan, D.C., Bonilla, C.A., 2015. Evaluation and improvement of the cligen model for storm and rainfall erosivity generation in central chile. Catena 127, 206–213. https://doi.org/10.1016/j.catena.2015.01.002.
Lützow, M.V., Kögel-Knabner, I., Ekschmitt, K., Matzner, E., Guggenberger, G., Marschner, B., Flessa, H., 2006. Stabilization of organic matter in temperate soils: Mechanisms and their relevance under different soil conditions – A review. Eur. J. Soil Sci. 57, 426–445. https://doi.org/10.1111/j.1365-2389.2006.00809.x.
Madhavan, D.B., Baldock, J.A., Read, Z.J., Murphy, S.C., Cunningham, S.C., Perring, M.P., Herrmann, T., Lewis, T., Cavagnaro, T.R., England, J.R., Paul, K.I., Weston, C.J., Baker, T.G., 2017. Rapid prediction of particulate, humus and resistant fractions of soil organic carbon in reforested lands using infrared spectroscopy. J. Environ. Manage. 193, 290–299. https://doi.org/10.1016/j.jenvman.2017.02.013.
Margenot, A.J., Calderón, F.J., Bowles, T.M., Parikh, S.J., Jackson, L.E., 2015. Soil organic matter functional group composition in relation to organic carbon, nitrogen, and phosphorus fractions in organically managed tomato fields. Soil Sci. Soc. Am. J. 79, 772. https://doi.org/10.2136/sssaj2015.02.0070.
Matus, F., Amigo, X., Kristiansen, S.M., 2006. Aluminium stabilization controls organic carbon levels in Chilean volcanic soils. Geoderma 132, 158–168. https://doi.org/10.1016/j.geoderma.2005.05.005.
Matus, F., Rumpel, C., Neculman, R., Panichini, M., Mora, M.L., 2014. Soil carbon storage and stabilisation in andic soils: a review. Catena 120, 102–110. https://doi.org/10.1016/j.catena.2014.04.008.
Moore, T.R., Trofymow, J.A., Prescott, C.E., Titus, B.D., 2011. Nature and nurture in the dynamics of C, N and P during litter decomposition in Canadian forests. Plant Soil 339, 163–175. https://doi.org/10.1007/s11104-010-0563-3.
Morrison, E.W., Pringle, A., van Diepen, L.T.A., Grandy, A.S., Melillo, J.M., Frey, S.D., 2019. Warming alters fungal communities and litter chemistry with implications for soil carbon stocks. Soil Biol. Biochem. Biochem. 132, 120–130. https://doi.org/10.1016/j.soilbio.2019.02.005.
Nelson, D.W., Sommer, L.E., 1982. Total Carbon, Organic Carbon and Organic Matter In: Pager, AL, RH Hiller and DR Keenay (ed.) Method of soil analysis, Part II, in: Am. Soc. of Agron. pp. 539–579.
Oades, J.M., 1984. Soil organic matter and structural stability: mechanisms and implications for management. Plant Soil 76, 319–337. https://doi.org/10.1007/BF02205590.
Parikh, S.J., Goyne, K.W., Margenot, A.J., Mukome, F.N.D., Calderón, F.J., 2014. Soil chemical insights provided through vibrational spectroscopy. Adv. Agron. 126, 1–148. https://doi.org/10.1016/B978-0-12-800132-5.00001-8.
Peltre, C., Bruun, S., Du, C., Thomsen, I.K., Jensen, L.S., 2014. Assessing soil constituents and labile soil organic carbon by mid-infrared photoacoustic spectroscopy. Soil Biol. Biochem. 77, 41–50. https://doi.org/10.1016/j.soilbio.2014.06.022.
Pfeiffer, M., Mascayano, C., Aburto, F., 2010. Soils of Chilean Patagonia in Glacial and Periglacial Environments. Eurasian Soil Sci. 43, 1430–1438. https://doi.org/10.1134/S106422931013003X.
Poirier, N., Sohi, S.P., Gaunt, J.L., Mahieu, N., Randall, E.W., Powlson, D.S., Evershed, R.P., 2005. The chemical composition of measurable soil organic matter pools. Org. Geochem. 36, 1174–1189. https://doi.org/10.1016/j.orggeochem.2005.03.005.
Post, W.M., Kwon, K.C., 2000. Soil carbon sequestration and land-use change: Processes and potential. Glob. Chang. Biol. 6, 317–327. https://doi.org/10.1046/j.1365-2486.2000.00308.x.
Ramírez, P., Calderón, F., Fonte, S., Bonilla, C., 2019. Environmental controls and long-term changes on carbon stocks under agricultural lands. Soil Tillage Res. 186, 310–321.
Romero, C.M., Engel, R.E., D'Andrilli, J., Chen, C., Zabinski, C., Miller, P.R., Wallander, R., 2018. Patterns of change in permanganate oxidizable soil organic matter from semiarid drylands reflected by absorbance spectroscopy and Fourier transform ion cyclotron resonance mass spectrometry. Org. Geochem. 120, 19–30. https://doi.org/10.1016/j.orggeochem.2018.03.005.
Roth, V.-N., Lange, M., Simon, C., Hertkorn, N., Bucher, S., Goodall, T., Griffiths, R.I., Mellado-Vázquez, P.G., Mommer, L., Oram, N.J., Weigelt, A., Dittmar, T., Gleixner, G., 2019. Persistence of dissolved organic matter explained by molecular changes during its passage through soil. Nat. Geosci. 12, 755–761. https://doi.org/10.1038/s41561-019-0417-4.
Rumpel, C., Rodríguez-Rodríguez, A., González-Pérez, J.A., Arbelo, C., Chabbi, A., Nunan, N., González-Vila, F.J., 2012. Contrasting composition of free and mineral-bound organic matter in top- and subsoil horizons of Andosols. Biol. Fertil. Soils 48, 411. https://doi.org/10.1007/s00374-011-0635-4.
Sadsawka, A., Carrasco, M., Grez, R., Mora, M., Flores, H., Neaman, A., 2006. Métodos de análisis recomendados para los suelos de. Chile. Ser. Actas INIA 163, N°34.
Sarker, T.C., Incerti, G., Spaccini, R., Piccolo, A., Mazzoleni, S., Bonanomi, G., 2018. Linking organic matter chemistry with soil aggregate stability: Insight from13C NMR spectroscopy. Soil Biol. Biochem. 117, 175–184. https://doi.org/10.1016/j.soilbio.2017.11.011.
Schmidt, M.W.I., Torn, M.S., Abiven, S., Dittmar, T., Guggenberger, G., Janssens, I.A., Kleber, M., Kögel-Knabner, I., Lehmann, J., Manning, D.A.C., Nannipieri, P., Rasse, D.P., Weiner, S., Trumbore, S.E., 2011. Persistence of soil organic matter as an ecosystem property. Nature 478, 49–56. https://doi.org/10.1038/nature10386.
Shen, C., Xiong, J., Zhang, H., Feng, Y., Lin, X., Li, X., Liang, W., Chu, H., 2013. Soil pH drives the spatial distribution of bacterial communities along elevation on Changbai Mountain. Soil Biol. Biochem. 57, 204–211. https://doi.org/10.1016/j.soilbio.2012.07.013.
Song, B., Niu, S., Zhang, Z., Yang, H., Li, L., Wan, S., 2012. Light and heavy fractions of soil organic matter in response to climate warming and increased precipitation in a temperate steppe. PLoS One 7, e33217. https://doi.org/10.1371/journal.pone.0033217.
Srivastava, P., Singh, R., Bhadouria, R., Tripathi, S., Singh, H., Raghubanshi, A.S., 2019. Understanding Soil Aggregate Dynamics and Its Relation With Land Use and Climate Change. In: Climate Change and Agricultural Ecosystems. Elsevier, pp. 331–354.
Strosser, E., 2010. Methods for determination of labile soil organic matter: An overview. J. Agrobiol. 27, 49–69. https://doi.org/10.2478/s10146-009-0008-x.
Summers, D., Lewis, M., Ostendorf, B., Chittleborough, D., 2011. Visible near-infrared reflectance spectroscopy as a predictive indicator of soil properties. Ecol. Indic. 11, 123–131. https://doi.org/10.1016/j.ecolind.2009.05.001.
Tan, Z., Lal, R., Owens, L., Izaurralde, R.C., 2007. Distribution of light and heavy fractions of soil organic carbon as related to land use and tillage practice. Soil Tillage Res. 92, 53–59. https://doi.org/10.1016/j.still.2006.01.003.
Tirol-Padre, A., Ladha, J.K., 2004. Assessing the reliability of permanganate-oxidizable carbon as an index of soil labile carbon. Soil Sci. Soc. Am. J. 68, 969–978. https://doi.org/10.2136/sssaj2004.9690.
Turchenek, L.W., Oades, J.M., 1979. Fractionation of organo-mineral complexes by sedimentation and density techniques. Geoderma 21, 311–343. https://doi.org/10.1016/0016-7061(79)90005-3.
UNEP, 1997. World Atlas of Desertification, Second. ed. United Nations Environment Programme, Arnold, London.
UNEP, 1992. World Atlas of Desertification, First. ed. United Nations Environment Programme, Arnold, London.
UNESCO, 2010. Atlas de Zonas Áridas de América Latina y el Caribe. Dentro del marco del proyecto "Elaboración del Mapa de Zonas Áridas, Semiáridas y Subhúmedas de América Latina y el Caribe". CAZALAC. Documentos Técnicos del PHI-LAC, No25.
Verma, B.C., Datta, S.P., Rattan, R.K., Singh, A.K., 2013. Labile and stabilised fractions of soil organic carbon in some intensively cultivated alluvial soils. J. Environ. Biol. 34, 1069.
Viscarra Rossel, R.A., Walvoort, D., McBratney, A., Janik, L., Skjemstad, J., 2006. Visible, near infrared, mid infrared or combined diffuse reflectance spectroscopy for

simultaneous assessment of various soil properties. Geoderma 131, 59–75. https://doi.org/10.1016/j.geoderma.2005.03.007.

Walkley, A., Black, I.A., 1934. An examination of the Degtjareff method for determining organic carbon in soils: Effect of variation in digestion conditions and of inorganic soil constituents. Soil Sci. 63, 251–263. https://doi.org/10.1097/00010694-194704000-00001.

Wardle, D.A., 1992. A comparative assessment of factors which influence microbial biomass carbon and nitrogen levels in soil. Biol. Rev. Camb. Philos. Soc. 67, 321–358. https://doi.org/10.1111/j.1469-185X.1992.tb00728.x.

Weil, R., Islam, K.R., Stine, M.A., Gruver, J.B., Samson-Liebig, S.E., 2003. Estimating active carbon for soil quality assessment: A simplified method for laboratory and field use. Am. J. Altern. Agric. 18, 3–17. https://doi.org/10.1079/ajaa2003003.

Wickings, K., Grandy, A.S., Reed, S.C., Cleveland, C.C., 2012. The origin of litter chemical complexity during decomposition. Ecol. Lett. 15, 1180–1188. https://doi.org/10.1111/j.1461-0248.2012.01837.x.

Wiesmeier, M., Urbanski, L., Hobley, E., Lang, B., von Lützow, M., Marin-Spiotta, E., van Wesemael, B., Rabot, E., Ließ, M., Garcia-Franco, N., Wollschläger, U., Vogel, H.J., Kögel-Knabner, I., 2019. Soil organic carbon storage as a key function of soils – A review of drivers and indicators at various scales. Geoderma 333, 143–162. https://doi.org/10.1016/j.geoderma.2018.07.026.

Yan, D., Wang, D., Yang, L., 2007. Long-term effect of chemical fertilizer, straw, and manure on labile organic matter fractions in a paddy soil. Biol. Fertil. Soils 44, 93–101. https://doi.org/10.1007/s00374-007-0183-0.